JOURNAL OF AIRCRAFT
Vol. 45, No. 2, March–April 2008

Wide Area Augmentation System-Based Flight Inspection System

Euiho Kim,* Todd Walter,† and J. David Powell‡
Stanford University, Stanford, California 94305

DOI: 10.2514/1.32531

The Federal Aviation Administration's augmentation to the global positioning system for civil aviation is called the wide area augmentation system. This paper introduces the wide area augmentation system-based flight inspection system. This system is better optimized than the current flight inspection systems in terms of accuracy, cost, and efficiency. Although they meet the Federal Aviation Administration's flight inspection system accuracy requirements, the current flight inspection systems are either higher cost or less efficient. The innovative use of the wide area augmentation system with a radar altimeter and a television positioning system without a requirement for an inertial navigator makes it possible for the wide area augmentation system-based flight inspection system to have low cost and high efficiency in flight inspection for instrument landing system calibration. The wide area augmentation system-based flight inspection system meets the Federal Aviation Administration's accuracy requirements for CAT III ILS calibration and also provides firm integrity algorithms. The performance of the wide area augmentation system-based flight inspection system is confirmed with tests using flight data taken in collaboration with the Federal Aviation Administration.

Nomenclature

b	=	range error due to reference position error
c	=	speed of light
I	=	ionospheric delay error
k	=	satellite vehicle number
l	=	line of sight vector
M	=	noise in code phase measurements
N	=	integer ambiguity
R	=	reference position index
r	=	distance between a receiver and a satellite
T	=	tropospheric delay error
t	=	time index during navigation
W	=	weighting matrix
X	=	receiver position and clock error vector
Y	=	time series of linearized difference of carrier phase measurements
y	=	linearized difference of carrier phase measurements
β	=	vector including the intercept and the slope
β_0	=	intercept in a first-order liner regression
β_1	=	slope in a first-order liner regression
$\hat{\beta}_{\mathrm{OLS}}$	=	estimated β using ordinary least squares
Γ	=	time series of code minus carrier phase measurements
$\Delta\hat{I}$	=	estimated ionospheric gradient
$\Delta(\cdot)$	=	difference of the same variable at two epochs
δt_s	=	satellite clock error
δt_u	=	receiver clock error
$\delta\bar{x}_{\mathrm{bias}}$	=	reference position bias vector
$\delta\bar{x}_{t,0}$	=	relative position vector between time t and 0
ε	=	noise in carrier phase measurements
$\tilde{\varepsilon}$	=	sum of noise and residual correction errors in carrier phase measurements
$\hat{\varepsilon}$	=	time series of the errors in the linearized difference of carrier phase measurements
ρ	=	code phase measurements
Φ	=	carrier phase measurements
Ψ	=	matrix of regressor variables
Ω	=	time series of noise in code phase measurements

Received 31 May 2007; revision received 30 August 2007; accepted for publication 2 September 2007.

*Ph.D. Candidate, Aeronautics and Astronautics; atomstan@stanford.edu.
†Senior Research Engineer, Aeronautics and Astronautics; twalter@stanford.edu.
‡Emeritus Professor, Aeronautics and Astronautics; jdpowell@stanford.edu.

I. Introduction

THE instrument landing system (ILS) is the primary landing guidance system in the United States. Therefore, the ILS must provide proper guidance at all times and at all installations. However, because of its sensitivity to multipath, the accuracy of an ILS may significantly degrade when there is a change in the local environment, for example, new construction near the ILS [1,2]. As a result, the ILS can provide an inaccurate landing course and cause a dangerous situation. For this reason, the Federal Aviation Administration (FAA) regularly checks and calibrates the ILS to maintain its accuracy.

The guidance of an ILS is checked through a flight inspection (FI). During an FI, an aircraft approaches a runway following the ILS guidance. The flight path during approach is determined by a flight inspection system (FIS), and the estimated flight path indicates the actual ILS guidance. This flight path is compared to the desired ILS guidance stored in a flight inspection system. If there is a deviation in the actual ILS guidance from the desired one, a calibration is required and performed by ground crews.

The first instrument used for the ILS calibration was a theodolite, an instrument that measures horizontal and vertical angles.[§] Figure 1 shows the old fashioned ILS calibration procedure with a theodolite. This procedure required very skilled people and was time consuming. Then, an automatic light or laser tracker replaced the manual theodolites around the 1970s–1980s. The light tracker followed a light source installed on the airplane, and the laser tracker followed its reflected signal from the airplane. Flight paths were still estimated on the ground, and the overall ILS calibration procedure took a significant amount of time. During the 1980s, the inertial-based automatic (or automated) flight inspection system (AFIS) was developed [3]. This system originally used a navigation grade inertial navigation system (INS) as a primary sensor with a barometric

[§]International Committee for Airspace Standards and Calibration's "Flight Inspection History" available online at http://avnwww.jccbi.gov/icasc/fi_history.html [retrieved 1 April 2007].

Fig. 1 The two surveyors on the ground measure the aircraft's deviation from the desired flight path using a theodolite (ILS Calibration by DC3, http://www.airwaysmuseum.com/DC3%20ILS%20calibration.htm [retrieved 13 December 2006]).

altimeter, a radar altimeter (RA), a camera system, and a pilot event button. More recently, the AFIS has been augmented with an unaided global positioning system (GPS) signal as well. A Kalman filter is used to estimate a flight trajectory by fusing the measurements from those sensors. This system is an automated self-contained system that made the ILS calibration procedure more efficient and convenient. However, the drawbacks of the inertial-based AFIS are high cost and degrading accuracy further from a runway. Also, an airplane needs to fly level over the whole runway to calibrate various biases in the INS. Regardless of the drawbacks, this kind of AFIS has continuously evolved and is being used by the United States and worldwide. A modern inertial-based AFIS is shown in Fig. 2.

Precise positioning techniques using differential GPS were developed and commercialized during the 1990s [4]; the techniques were adapted to a flight inspection system for the ILS calibration problem. This kind of FIS is called the differential GPS-based automatic flight inspection system (DGPS-based AFIS). This system usually provides centimeter level accuracy in real time without any drifts. However, it requires a time-consuming procedure in setting up a local reference station in each airport, which is the main drawback of the DGPS-based AFIS.

The current automated flight inspection systems are the inertial-based AFIS and DGPS-based AFIS, whose characteristics are quite different in terms of cost, accuracy, and efficiency. In the United States, the FAA prefers to use the inertial-based AFIS mainly due to its efficiency despite of the higher cost. To complete the airborne inspection of numerous ILSs around the United States in a limited time, efficiency is the most important factor. Previously, in an effort to replace the inertial-based AFIS with a lower cost system, wide area augmentation system-aided flight inspection system (WAAS-aided FIS) was proposed [5]. This system uses a lower grade INS, WAAS, a radar altimeter, and a television positioning system (TVPS). The advantages of this system are lower cost, better efficiency, and better accuracy than the inertial-based AFIS. Also, the WAAS-aided FIS can be easily implemented in the inertial-based AFIS due to the similarity of these two systems. However, the drawback of this system is that it has some vulnerability to a possible accuracy degradation in rare events, such as a sharp ionospheric gradient or severe multipath, because it is constrained to only use standard positioning outputs from the WAAS receiver.

Through continuing efforts to replace the inertial-based AFIS with a lower cost system, we introduce the WAAS-based FIS in this paper. The WAAS-based FIS is a self-contained system equipped with a single frequency WAAS receiver, a radar altimeter, and a television positioning system. A specialized positioning algorithm called a time-differenced precise relative positioning (TDPRP) method is used for this system. The positioning algorithm uses the difference of carrier phase measurements at two epochs as ranging sources and uses WAAS correction messages. Taking advantage of the small lag in positioning that is allowed in flight inspection, TDPRP uses smoothed WAAS fast-clock corrections and eliminates relative ionospheric delays at the two epochs. Not only does the WAAS-based FIS provide an accurate position that meets flight inspection system accuracy requirements, its integrity is also affirmed by the WAAS integrity messages and further safety checks. Those checks include an ionospheric delay compensation and the validation of a reference position from a radar altimeter and a TVPS. Overall, the WAAS-based FIS overcomes the shortcomings of the other FISs and provides the optimized performance in the aspects of accuracy, cost, efficiency, and integrity.

This paper is organized as follows. First, the nature of the ILS calibration problem and its accuracy requirements are briefly introduced. Then, the details of the proposed WAAS-based FIS are discussed, including its system architecture, positioning algorithm, ionospheric delay compensation technique with a single frequency receiver, satellite exclusion tests, WAAS fast-clock correction filtering, and validation of a reference position from a radar altimeter and a TVPS. Thirdly, the test results from implementing the WAAS-based FIS with flight-test data are presented. Lastly, the conclusions are provided.

II. ILS Calibration Problem and Flight Inspection System Accuracy Requirements

The ILS consists of a glide slope, a localizer, and marker beacons. A localizer and a glide slope provide horizontal and vertical guidance to a runway. Marker beacons alert a pilot to his/her approaching specific way points with an audible alert. Therefore, the guidance from a glide slope and a localizer is the main objective for the ILS calibration in flight inspection.

The ILS calibration problem is unique among other estimation problems. First, the aircraft's trajectory may be estimated in near real time, that is, within a few minutes of real time. Second, the surveyed runway threshold position can be used to estimate flight paths during approach and, indeed, is being used in the inertial-based AFIS. Therefore, a flight inspection procedure using these features, as with the inertial-based AFIS, can have two modes as illustrated in Fig. 3: approach mode and flight trajectory estimation and ILS calibration mode. The duration of the approach mode is usually less than a few minutes. Therefore, only a short set of measurements is available. The accuracy required for the flight inspection system is not rectilinear. Because the ILS is an angular guidance system, the accuracy requirements of a flight inspection system are also angular. The FAA uses the following guidelines. For a CAT I ILS, an estimation error should be less than 0.05 deg from the glide slope and localizer antennas but not less than 30 cm in vertical and 60 cm in cross track. For a CAT II/III ILS, an estimation error should be less than 0.015 deg from the glide slope and localizer antennas but not

Fig. 2 Modern computerized FIS (JCAB Gulfstream IV flight inspection system, www.nxt-afis.com/products_home.htm [retrieved 5 April 2007]).

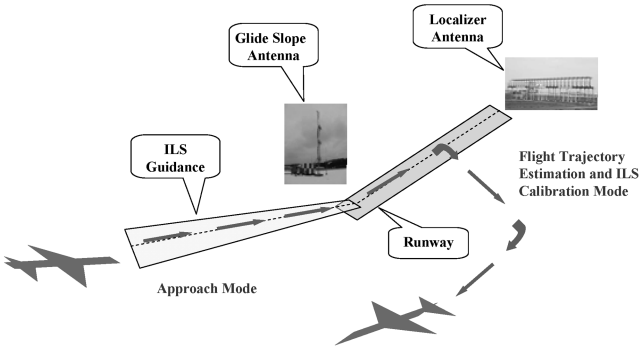

Fig. 3 Two flight inspection modes in ILS calibration.

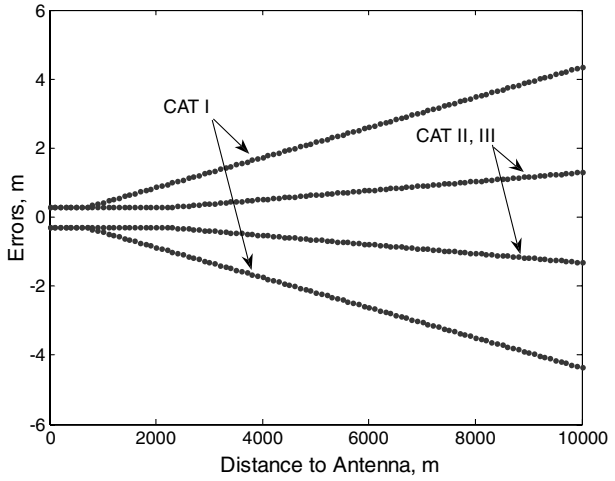

Fig. 4 Vertical flight inspection system accuracy requirements for ILS calibration.

less than 30 cm in vertical and 60 cm in cross track. In other words, the accuracy requirements become looser as the distance from those antennas increases. The vertical flight inspection system accuracy requirements for ILS calibration are shown in Fig. 4.

III. WAAS-Based Flight Inspection System

This section discusses the details of the WAAS-based FIS. The overall architecture and its specific positioning algorithms are presented. Also, integrity features in this system are addressed.

A. Why Use WAAS for ILS Calibration?

The WAAS is an augmentation system of the GPS in the United States. It was developed by the FAA to serve various phases of flight operation, for example en route, nonprecision, and precision approaches, as a primary means of navigation in the United States. WAAS became operational in 2003 and can guide an airplane down to within 200 ft above an airport's runway as of 2007. The principles of WAAS are extensively discussed in [6,7].

The current WAAS 95% accuracy is better than 0.935 m in horizontal and 1.289 m in vertical [8], which does not meet the ILS calibration accuracy requirements. Therefore, the WAAS cannot be directly used for the ILS calibration problem. However, the WAAS still has useful features. First, the WAAS broadcasts accurate correction messages for GPS satellite clock, ephemeris, and ionospheric delay errors. Secondly, the WAAS issues a flag when satellite anomalies and severe ionospheric disturbances occur [9]. These features play a very important role in helping the WAAS-based FIS have sound position solutions and firm integrity.

B. System Architecture

The WAAS-based FIS is a system that has a single frequency WAAS receiver, a radar altimeter, a TVPS, and a computer. No information from an INS is required. The same kinds of radar altimeter and TVPS used in the current inertial-based AFIS are used in the WAAS-based FIS. The 95% accuracy of the radar altimeter is better than 15 cm [10]. The 95% accuracy of the TVPS is better than 15 cm in cross track and 30 cm in along track.¶ This integrated system is optimally designed for the ILS calibration problem in terms of accuracy, cost, efficiency, and integrity.

Figure 5 illustrates the overall algorithm of the WAAS-based FIS. During approach, WAAS position and raw GPS/WAAS measurements are collected. The GPS/WAAS measurements include ephemeris, L1 code and carrier phase measurements, and WAAS messages. The ephemeris parameters provide GPS satellite locations at a specific time. L1 code and carrier phase measurements provide range information between a user and satellites. The WAAS

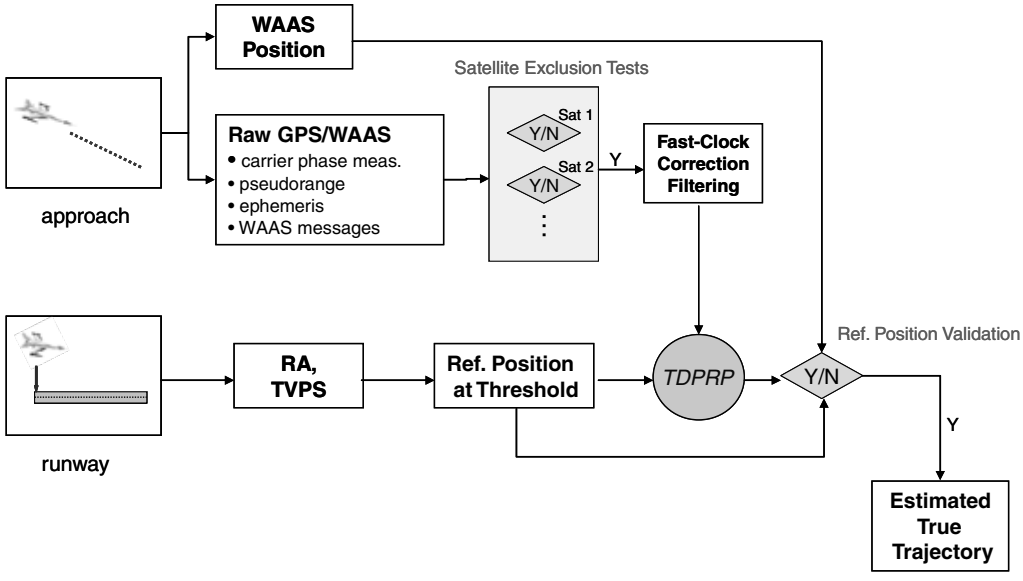

Fig. 5 System architecture of WAAS-based FIS.

¶Television Positioning System, NXT, available online at http://www.nxt-afis.com/television_positioning_system.html [retrieved 1 April 2007].

messages provide GPS error corrections and satellite health. Over the threshold of a runway, the radar altimeter measures the vertical distance between the airplane and the runway threshold. At that point, the TVPS measures the cross-track and along-track deviations of the airplane from the center line and the threshold mark of the runway by using its camera images. The effect of an airplane's attitude on the radar altimeter and the TVPS at the threshold is corrected with a proprietary filter in the current inertial-based AFIS. Because the position of the threshold is accurately surveyed, the radar altimeter and the TVPS provide an accurate instant 3-D position of the airplane over the threshold. A specialized positioning algorithm, the TDPRP method, uses this reference position and the raw measurements to compute precise relative positions. The estimated flight trajectory during approach is obtained by adding the relative positions to the reference position. The detailed algorithm of the TDPRP will be discussed in Sec. III.C. There are two integrity features for the soundness of the estimated flight trajectory: satellite exclusion tests and validation of the reference position from the radar altimeter and the TVPS. Satellite exclusion tests are implemented to discard a satellite that should not be used in TDPRP for various reasons. The integrity of a reference position from a radar altimeter and a TVPS is checked using both the WAAS position during approach and the precise relative position from the TDPRP. Even though this validation test is limited to the level of WAAS accuracy, it is useful when a radar altimeter or a TVPS introduces an abnormally large error. The two integrity features will be further discussed later in this section.

C. Time-Differenced Precise Relative Positioning

The difference of carrier phase measurements at two epochs has been proposed as a source for velocity and relative position [11,12]. The formulation used in [11,12] is essentially the same, but Graas and Soloviev [11] used it for precise velocity estimation and Somerville and Raquet [12] used it to obtain relative position. The TDPRP proposed in this paper uses the same formulation and also computes relative positions with a single frequency receiver. However, the main difference from the previous approaches is that the ionospheric delay gradient at two epochs is estimated and removed using the combination of L1 code and carrier phase measurements in near real time. The ionospheric delay gradient estimation with a single frequency receiver was recently introduced in [13] and will be briefly discussed in Sec. III.D.

Carrier phase measurements from a GPS satellite have the following expression in units of length.

$$\Phi = r + c[\delta t_u - \delta t_s] - I + T + N + \varepsilon \tag{1}$$

where r is the true range between a receiver and a satellite, c is the speed of light, and δt_u and δt_s are the receiver and satellite clock errors, respectively. I is an ionospheric delay in L1 frequency and T is a tropospheric delay. N is an integer ambiguity and ε includes multipath, thermal noises, and modeling errors in the carrier phase measurements.

Assuming that there is no cycle slip, a single difference of carrier phase measurements from a satellite k at two epochs, t and 0, is as follows:

$$\Phi_t^k - \Phi_0^k = r_t^k - r_0^k + c\Delta t_u - c\Delta t_s^k - \Delta I_t^k + \Delta T_t^k + \Delta \varepsilon_t^k \tag{2}$$

where $\Delta(\cdot)$ is the difference of the same variable at the two epochs.

Now, applying WAAS satellite clock-ephemeris error corrections and tropospheric error corrections to Eq. (2) and linearizing it with respect to a reference position, Eq. (2) becomes, with a short base line assumption,

$$\begin{aligned} y_{t,0}^k &= r_t^k - r_0^k - \left(\hat{r}_{R,t}^k - \hat{r}_{R,0}^k\right) + c\Delta t_u - \Delta I_t^k + \Delta \tilde{\varepsilon}_t^k \\ &= -1_t^k \cdot \delta \bar{x}_{t,0} + c\Delta t_u + b_{\mathrm{Ref},t}^k - \Delta I_t^k + \Delta \tilde{\varepsilon}_t^k \end{aligned} \tag{3}$$

where $\hat{r}_R^k$ is the computed distance between the satellite k and a reference position using the broadcast ephemeris, 1_t^k is a line-of-sight vector to the satellite k at time t, $\delta \bar{x}_{t,0}$ is a relative position of a receiver from the position at time 0, $b_{\mathrm{Ref},t}$ is an error caused from the imperfect knowledge of reference position at time t, and $\Delta \tilde{\varepsilon}_t^k$ includes residual correction errors and higher order modeling errors due to linearization in addition to $\Delta \varepsilon_t^k$.

It is helpful to understand the error characteristics of Eq. (3) to see why this formulation is used in the WAAS-based FIS. Because $c\Delta t_u$ is common to all satellites, it should be easily estimated. Therefore, the error sources in Eq. (3) are $b_{\mathrm{Ref},t}$, ΔI, and $\Delta \tilde{\varepsilon}$.

Now, let us assume that we know satellite locations perfectly to see the sole effects of reference position errors. When the exact reference position is known, $b_{\mathrm{Ref},t}$ is zero. However, when the reference position has some errors, the computed distance between the satellite k and a reference position has the following expression:

$$\hat{r}_{R,t}^k = r_{R,t}^k + 1_t^k \cdot \delta \bar{x}_{\mathrm{bias}} \tag{4}$$

where $\delta \bar{x}_{\mathrm{bias}}$ is a reference position error vector from a true position to the erroneous reference position.

Then,

$$r_t^k - \hat{r}_{R,t}^k \approx -1_t^k \cdot \delta \bar{x}_{t,0} - 1_t^k \cdot \delta \bar{x}_{\mathrm{bias}} - r_0^k + \hat{r}_{R,0}^k \approx 1_0^k \cdot \delta \bar{x}_{\mathrm{bias}} \tag{5}$$

Therefore, $b_{\mathrm{Ref},t}^k$ is

$$b_{\mathrm{Ref},t}^k \approx -1_t^k \cdot \delta \bar{x}_{\mathrm{bias}} + 1_0^k \cdot \delta \bar{x}_{\mathrm{bias}} \tag{6}$$

From Eq. (6), we can see that $b_{\mathrm{Ref},t}^k$ is small when t is near zero and increases as t increases.

Next, ΔI is estimated and removed by using the difference of L1 code and carrier phase measurements, assuming that ΔI behaves linearly during approach. More details of the estimation of ΔI will be discussed in Sec. III.D.

$\Delta \tilde{\varepsilon}_t^k$ includes tropospheric delay correction residuals, satellite clock-ephemeris correction residuals, multipath, modeling errors, thermal noise, and so on. $\Delta \tilde{\varepsilon}_t^k$ is also very small when t is near zero and increases as t increases because the residual correction errors are highly correlated [14,15]. Fortunately, multipath and other receiver related noise are small enough ($\sim$1 or 2 cm) for our application.

Overall, the error characteristic of the single difference of the carrier measurements is that the error is very small when t is near zero and grows over time. This error characteristic is well suited for the ILS calibration problem because the allowable error limits also increase as t increases. Once ΔI is removed, the level of error that grows over time is insignificant for the ILS calibration problem.

Finally, a set of linear equations can be formed as follows:

$$\underbrace{\begin{bmatrix} y_{t,0}^1 \\ y_{t,0}^2 \\ \vdots \\ y_{t,0}^n \end{bmatrix}}_{Y} = \underbrace{\begin{bmatrix} -1_t^1 1 \\ -1_t^2 1 \\ \vdots \\ -1_t^k 1 \end{bmatrix}}_{G} \underbrace{\begin{bmatrix} \delta \bar{x}_{t,0} \\ C\Delta t_u \end{bmatrix}}_{X} + \underbrace{\begin{bmatrix} \hat{\varepsilon}_t^1 \\ \hat{\varepsilon}_t^2 \\ \vdots \\ \hat{\varepsilon}_t^k \end{bmatrix}}_{\hat{\varepsilon}} \qquad Y = GX + \hat{\varepsilon} \tag{7}$$

where $\hat{\varepsilon}$ includes $b_{\mathrm{Ref},t}$, $\Delta \tilde{\varepsilon}_t$, and residual errors from the compensation of ΔI.

Then, the relative position from TDPRP with respect to the reference position is computed using weighted least squares, as follows:

$$X = (G^T W^{-1} G)^{-1} G^T W^{-1} Y \tag{8}$$

where W is a weighting matrix. It is difficult to find W because some of the errors in Y are highly correlated over time. However, the overall errors have a dependency on the satellite elevation angle because the measurements from a GPS satellite with low elevation angles have large atmospheric delays and multipath. Therefore, a reasonable choice for the elements of the weighting matrix would be the sine of the satellite elevation angle.

D. Ionospheric Delay Gradient Estimation Using Linear Regression with a Single Frequency Receiver

This subsection gives a brief review of the ionospheric delay gradient estimation with a single frequency receiver introduced in [13]. The estimated ionospheric delay gradient is used to make a correction for the differential ionospheric delays between a reference position and any points during approach, which makes the WAAS-based FIS robust to various ionospheric effects with a single frequency receiver.

The basic measurements from a GPS satellite are code and carrier phase measurements. The carrier phase measurement is already expressed in Eq. (1). The code phase measurements, ρ, can be written in units of length as follows:

$$\rho = r + c[\delta t_u - \delta t_s] + I + T + M \tag{9}$$

where M includes multipath, thermal noises, and modeling errors in the code phase measurement.

The code minus carrier phase measurement at time t is

$$\rho_t - \Phi_t = 2I_t - N + M_t - \varepsilon_t \tag{10}$$

This difference includes ionospheric delays multiplied by two, an integer ambiguity, and noise in code and carrier phase measurements. Our interest here is to estimate a slant ionospheric delay rate. It should be noted that the ionospheric delays slowly change with respect to time during nominal ionospheric days. Therefore, the rate can be seen as a constant during a short time window (minutes). Assuming a constant ionospheric delay rate, Eq. (10) can be rewritten as

$$\rho_t - \Phi_t = \beta_0 + 2t \cdot \beta_1 + M_t - \varepsilon_t \approx \beta_0 + 2t \cdot \beta_1 + M_t \tag{11}$$

In Eq. (11), ε_t is ignored because it is much smaller than M_t.

Expressing the time series of Eq. (11) in a matrix form yields

$$\underbrace{\begin{bmatrix} \rho_{t_0} - \Phi_{t_0} \\ \rho_{t_1} - \Phi_{t_1} \\ \vdots \\ \rho_{t_n} - \Phi_{t_n} \end{bmatrix}}_{\Gamma} = \underbrace{\begin{bmatrix} 1 & 2 \cdot t_0 \\ 1 & 2 \cdot t_1 \\ & \vdots \\ 1 & 2 \cdot t_n \end{bmatrix}}_{\Psi} \underbrace{\begin{bmatrix} \beta_0 \\ \beta_1 \end{bmatrix}}_{\beta} + \underbrace{\begin{bmatrix} M_{t_0} \\ M_{t_1} \\ \vdots \\ M_{t_n} \end{bmatrix}}_{\Omega} \tag{12}$$

$$\Gamma = \Psi\beta + \Omega$$

Now, the problem becomes finding β in the presence of Ω. If Ω is white noise, the ordinary least squares is the best estimator. Fortunately, airborne multipath is very close to white noise [13]. Therefore,

$$\hat{\beta}_{\mathrm{OLS}} = (\Psi^T\Psi)^{-1}\Psi^T\Gamma \tag{13}$$

Once we have the estimated ionospheric delay gradient, $\hat{\beta}_1$, the differential ionospheric delay correction between a reference position and any points during approach is simply

$$\Delta\hat{I}_{t,0} = t \cdot \hat{\beta}_1 \tag{14}$$

It is interesting to see how useful the estimated ionospheric delay gradient is even during ionospheric nominal days. Figure 6 compares relative positions from implementing the TDPRP with and without compensating for the differential ionospheric delays using static experimental receiver data. The error was reduced and better centered around zero.

E. Satellite Exclusion Tests

To ensure safe position solutions from the TDPRP, it is necessary to detect any threats and exclude them. This section discusses how to choose the right set of satellites for the TDPRP using the WAAS integrity messages and other internal sanity check procedures.

Figure 7 shows a chart of the items that should be checked before including a satellite in the TDPRP. The first safety check is to see if

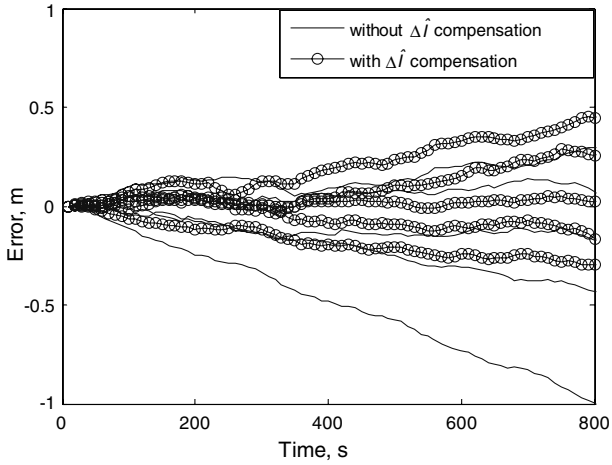

Fig. 6 Example of the effectiveness of applying $\Delta\hat{I}$ based on the measurement taken on 05 September 2005 at Stanford University.

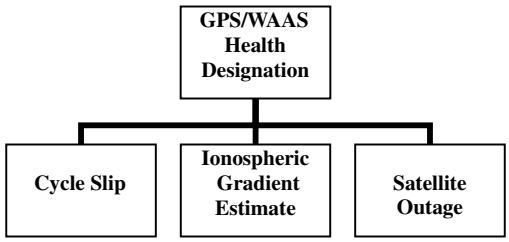

Fig. 7 Chart of items for satellite exclusion criteria.

there are any GPS/WAAS unhealthy or WAAS unmonitored designations. If these messages are delivered from GPS/WAAS for a particular satellite, that satellite will be excluded. Similarly, a satellite having a user differential range error indicator greater than or equal to 12 will be excluded as well because that satellite may have some problem and cannot be used for a WAAS-based precision approach [16].

Any satellite experiencing a cycle slip during approach is also excluded because the TDPRP must use continuously accumulated carrier phase measurements. In addition, the goodness of fit for the estimation of the ionospheric delay gradient must be examined. Any ionospheric delay gradients showing a severe nonlinear behavior can be detected by analyzing the residuals after fitting a first-order linear model on the code minus carrier phase measurements. Chi-square tests are a good indicator for goodness of fit [17]. Lastly, it is best to use the same set of satellites during the entire approach. A different set of satellites may introduce a sudden jump in relative positions, which is very undesirable for our application.

F. Fast-Clock Correction Filtering

Interestingly, WAAS positions typically have a 12-s periodic noise [5]. The main source of this periodic noise is fast-clock correction messages and range rate corrections (RRC). The broadcast fast-clock correction has a 0.125-m resolution and often shows an oscillatory pattern with a 12-s period. The fast-clock correction message must be filtered to result in smooth position solutions. Fortunately, the RRC can be easily turned off by setting it to zero in the receiver, which is advisable now that selective availability is turned off.

Figure 8 shows a typical example of the broadcast fast-clock corrections and smoothed fast-clock corrections. The smoothing process takes place after receiving all the messages during approach. Because the message has a 12-s periodic pattern for a considerable amount of time, a noncausal moving average filter having a 12-s length, or a multiple of 12 s, will remove the periodic pattern.

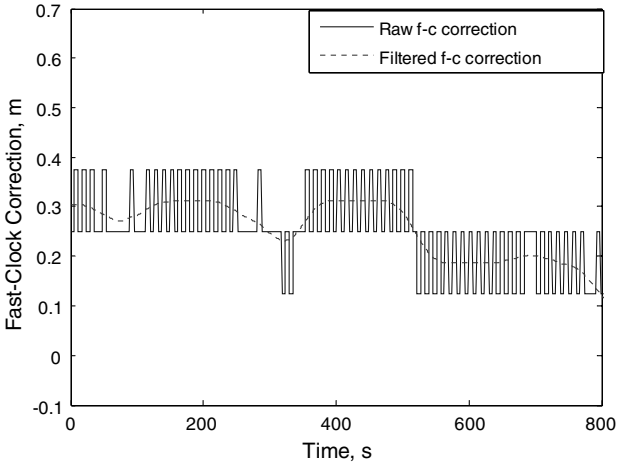

Fig. 8 Example of fast-clock correction filtering.

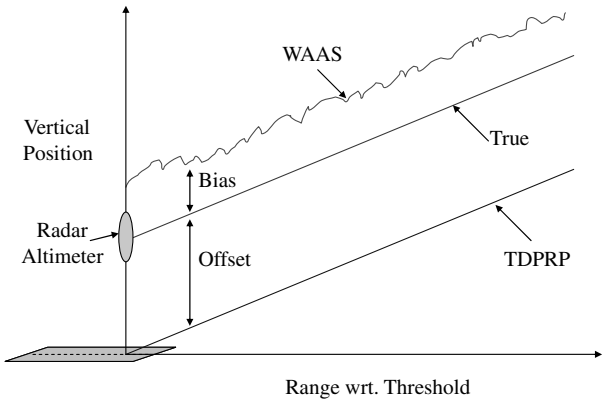

Fig. 9 Schematics of the characteristics of three position measurements (RA, WAAS, TDPRP) with true position.

G. Validation of a Reference Position from Radar Altimeter and TVPS

The radar altimeter and the TVPS provide the reference position over the threshold. Because the estimated flight path is the sum of the reference position and the relative position from the TDPRP, accurate measurements from those sensors are extremely important. This subsection discusses how to validate the reference position using the WAAS position.

Figure 9 depicts how a true flight trajectory is related to the WAAS position and the relative position from the TDPRP in the vertical. Basically, the WAAS position has a constant bias and noise on top of the true position during approach [5]. On the other hand, the position from the TDPRP is precise but has an offset to the true position. In mathematical expression, these positions can be described as follows:

$$\text{WAAS} = \text{true} + \text{bias} + \text{noise}, \qquad \text{TDPRP} = \text{true} - \text{offset} \quad (15)$$

Taking the average of the difference of the WAAS position and the TDPRP position during approach yields the following expression:

$$\text{AVG}_{(\text{WAAS}-\text{TDPRP})} = \frac{1}{n}\sum_{t=0}^{n}(\text{WAAS} - \text{TDPRP})_t \approx \text{bias} + \text{offset} \quad (16)$$

In Eq. (16), the noise in the WAAS position is averaged out to near zero.

Now, an instantaneous measurement of a radar altimeter over the threshold has an offset and a small error as follows:

$$\text{radar altimeter} = \text{true}_{\text{thr}} + \text{error} \quad (17)$$

The difference of the measurements of a radar altimeter and TDPRP over the threshold is

$$\Delta_{(\text{RA}-\text{TDPRP}_{\text{thr}})} = \text{radar altimeter} - \text{TDPRP}_{\text{thr}} = \text{error} + \text{offset} \quad (18)$$

Then, if we subtract Eq. (18) from Eq. (16), the remaining term is approximately the sum of the WAAS bias and the small error from the radar altimeter as follows:

$$\text{AVG}_{(\text{WAAS}-\text{TDPRP})} - \Delta_{(\text{RA}-\text{TDPRP}_{\text{thr}})} \approx \text{bias} - \text{error} \quad (19)$$

The message from Eq. (19) is that once we know the statistical distributions of the WAAS bias and the errors from a radar altimeter, which were already presented in the previous sections, we can also form a distribution of Eq. (19). Using this distribution, it is possible to check where the value of Eq. (19) stands on the distribution for each approach. If the value is beyond a threshold, for example 95% with a two-sided Gaussian distribution, a flag is raised to indicate a possible corruption in the radar altimeter measurement. A similar procedure can be used in horizontal with a TVPS. Considering the 95% accuracies of the WAAS, a radar altimeter, and a TVPS, the thresholds (2σ) are 1.11 m in horizontal and 1.3234 m in vertical, respectively.

IV. Flight-Test Results

For the validation of the WAAS-based FIS, the algorithm was tested with flight data taken during 30–31 October 2006 in collaboration with the FAA at Oklahoma City. During the flight test, DGPS positions from a real-time kinematic (RTK) system were also collected in addition to raw GPS/WAAS data. Current state-of-the-art RTK systems typically result in a few centimeter level of accuracy [18]. Therefore, the DGPS positions were used as a truth source for the validation of the WAAS-based FIS. A radar altimeter and a TVPS were not used because there were some hardware difficulties during the tests and so the reference positions were provided from the DGPS and the validation of the reference positions was not implemented.

Figure 10 shows an example of flight paths during the flight tests in east, north, and up coordinates with respect to the runway threshold. The total number of approaches used in this test is 23.

A. TDPRP Tests

Figures 11 and 12 show the horizontal and vertical errors from implementing the TDPRP with a reference position given from a DGPS position. The two pairs of the straight lines in these figures are the flight inspection system accuracy requirements for CAT I and CAT II/III ILS calibration. Note that the system accuracy requirements presented here differ from those in Fig. 4 because the horizontal guidance (localizer) antenna is located at the opposite end of the runway from the arrival threshold.

Figures 11 and 12 do not represent the total errors of the WAAS-based FIS tests because the reference position errors are not included.

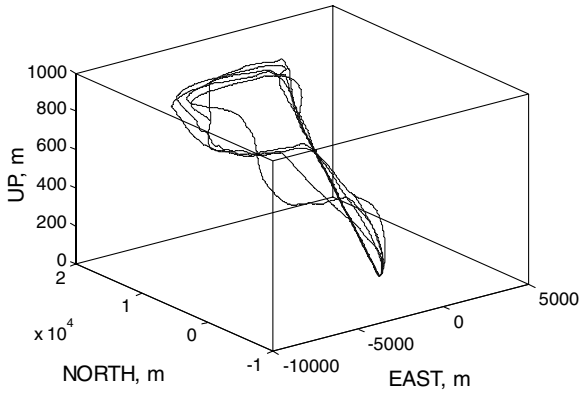

Fig. 10 Some of the flight trajectories in flight tests taken during 30–31 October 2006 at Oklahoma City.

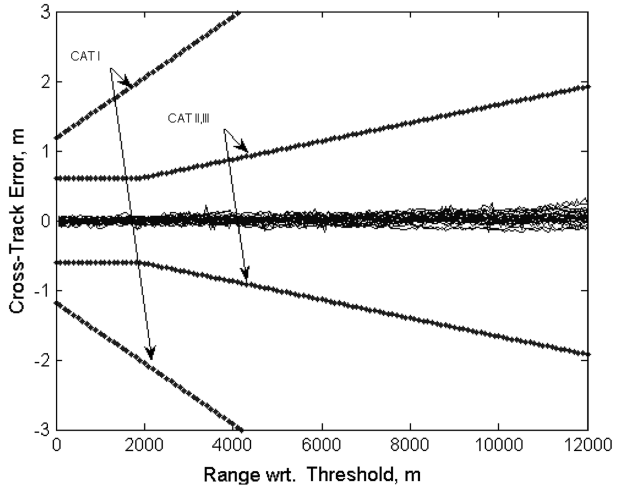

Fig. 11 Cross-track errors in meters of 23 approaches from the WAAS-based FIS (without TVPS errors).

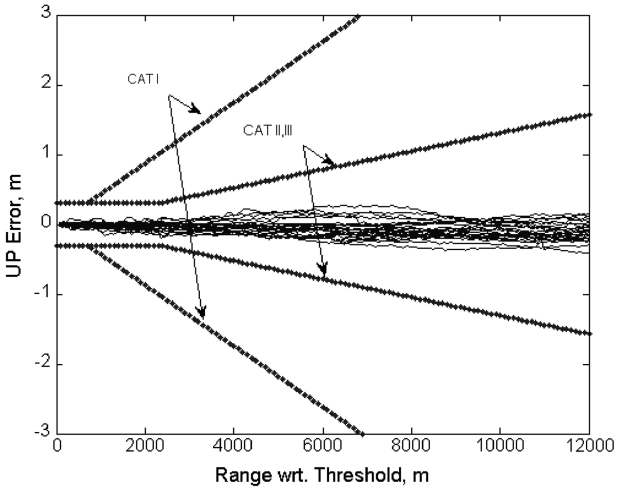

Fig. 12 Vertical error in meters of 23 approaches from the WAAS-based FIS (without RA errors).

However, these results clearly show the error characteristics of the TDPRP, which slowly increase over time. It is possible to predict the performance of the WAAS-based FIS using 95% accuracies of a radar altimeter and a TVPS.

B. WAAS-Based FIS Performance

To see the accuracy of the WAAS-based FIS, we should consider the total errors caused by both the TDPRP and the reference position error. Considering the errors from the TDPRP and the accuracy requirements for CAT II/III ILS, the most critical regions are around 2200 and 2000 m from the threshold in vertical and horizontal, respectively. The error distribution of the TDPRP in the critical regions is important because the total error, the sum of the errors from TDPRP and reference position errors, most likely violate the flight inspection system accuracy requirements for CAT II/III ILS calibration at that location. Table 1 summarized the statistics of the errors from the TDPRP at the critical regions.

Treating the TDPRP errors and reference position errors as independent random variables with zero mean, which is not exactly true but practically good enough, the distributions of the total errors can be easily calculated. Because the accuracies (95%) of a radar altimeter and a TVPS in cross track are about 15 cm, the total errors at the critical regions have 9.06-cm standard deviation in vertical and 8.55-cm standard deviation in cross track. It should be noted that a TVPS along-track error does not significantly effect the total error in vertical because the aircraft's descending angle is around 3 deg. Therefore, the 95% accuracy of the WAAS-based FIS is 18.12 cm in vertical and 17.10 cm in cross track at the critical regions. Therefore, the WAAS-based FIS sufficiently meets the flight inspection system accuracy requirements up to CAT II/III ILS calibration, whose limits are about 30 cm in vertical and 60 cm in cross track.

Table 1 Statistics of the TDPRP errors at critical regions

	Up, m	Cross track, m
Mean	−0.035	0.002
Std.	0.051	0.041
RMS	0.061	0.041

On the other hand, the critical region for a CAT I ILS cross-track calibration is at the threshold, and the accuracy requirement is 1.2 m at that location. In this case, the contribution of the TDPRP cross-track errors to the total error is negligible because the CAT I ILS cross-track requirement rapidly relaxes as the range from the threshold increases. Therefore, because 95% horizontal WAAS accuracy is 0.935 m, the total error of the system that would result by using the WAAS for the cross-track reference point determination (no TVPS required) would be well below the CAT I ILS requirement.

V. Conclusions

In this paper, the WAAS-based FIS is introduced. Its system architecture, positioning algorithm, and integrity features are thoroughly discussed. For the validation of the WAAS-based FIS algorithm, this system was tested with flight-test data taken during 30–31 October 2006 at Oklahoma City. The results were shown to meet the required accuracy for flight inspection of CAT I, II, and III ILS calibrations. For a CAT I ILS calibration, the system consists of a WAAS receiver and a radar altimeter. For CAT II and III ILS calibrations, the system also requires a TVPS.

Overall, the WAAS-based FIS provides more optimized performance than the other flight inspection systems in terms of accuracy, cost, efficiency, and integrity. Its accuracy is between the inertial-based AFIS and the DGPS-based AFIS, and its cost is significantly lower than either because there is no need for an INS or a DGPS ground reference station. The efficiency of the WAAS-based FIS outperforms the other two AFISs because it does not need personnel to install a reference station on the ground nor does it require the FI aircraft to fly level over the whole runway. The WAAS-based FIS also provides secure redundant integrity features using the WAAS messages and internal safety checks. It should be noted, however, that the scheme does require that modifications be made to a certified WAAS receiver.

Acknowledgments

The authors gratefully acknowledge the support of the FAA flight inspection division, Aviation System Standards (AVN), and extensive help from Uri Peled in the earlier stages of the research.

References

[1] Kayton, M., and Walter, F., *Avionics Navigation Systems*, 2nd ed., Wiley, New York, 1997, p. 619.

[2] Poulose, M. M., and Mahapatra, P. R., "ILS Glideslope Evaluation for Imperfect Terrain," *Proceedings of IEEE Transactions on Aerospace and Electronic Systems*, Vol. 24, No. 2, March 1988, pp. 186–191.

[3] Scherzinger, B. M., and Feit, C. M., "The Design, Simulation, and Implementation of an Accurate Positioning System for Automatic Flight Inspection System," *Proceedings of IEEE PLANS 1990*, IEEE, Piscataway, NJ, 1990, pp. 444–451.

[4] Feit, C. M., and Bates, M. R., "Accurate Positioning in a Flight Inspection System Using Differential Global Navigation Satellite Systems," *Proceedings of the ION International Technical Meeting*, Institute of Navigation, Fairfax, VA, pp. 955–964; also Institute of Navigation Paper GPS-94.

[5] Kim, E., Peled, U., Walter, T., and Powell, J. D., "A Development of WAAS-Aided Flight Inspection System," *IEEE/ION PLANS 2006 on Disc* [CD-ROM], IEEE/Institute of Navigation, San Diego, CA, 2006.

[6] Enge, P., Walter, T., Pullen, S., Kee, C., Chao, Y. C., and Tsai, Y. J., "Wide Area Augmentation of the Global Positioning System," *Proceedings of the IEEE*, Vol. 84, No. 8, Aug. 1996, pp. 1063–1088. doi:10.1109/5.533954

[7] Walter, T., and Enge, P., "The Wide-Area Augmentation System," *EGNOS-The European Geostationary Navigation Overlay System-A cornerstone of Galileo*, edited by J. ventura-Traveset, and D. Flament, European Space Agency Publications, Noordwijk, The Netherlands, Dec. 2006, pp. 395–411.

[8] NSTB/WAAS T&E Team, "Wide-Area Augmentation System Performance Analysis Report," Federal Aviation Administration William J. Hughes Technical Center, Atlantic City International Airport, NJ, (updated reports issued every quarter) http://www.nstb.tc.faa.gov/ArchiveList.html [retrieved 5 Nov. 2006].

[9] Klobuchar, J., "Ionospheric Effects on GPS," *Global Positioning System: Theory and Applications*, edited by B. Parkinson, and J. Spilker, Vol. 1, Progress in Astronautics and Aeronautics, AIAA, Reston, VA, 1996, pp. 485–515.

[10] Peled, U., "Radar Altimeter Evaluation-Refined Runway Data," Internal Report, Stanford, California, 28 May 2005.

[11] Graas, F. V., and Soloviev, A., "Precise Velocity Estimation Using a Stand-Alone GPS Receiver," *ION NTM 2003 on Disc* [CD-ROM], Institute of Navigation, Anaheim, CA, 2004.

[12] Somerville, E. M., and Raquet, J. F., "Self-Differential GPS—What are the Limits?," *ION NTM 2006 on Disc* [CD-ROM], Institute of Navigation, Monterey, CA, 2006.

[13] Kim, E., Walter, T., and Powell, J. D., "Adaptive Carrier Smoothing using Code and Carrier Divergence," *ION NTM 2007 on Disc* [CD-ROM], Institute of Navigation, San Diego, CA, 2007.

[14] Walter, T., Hansen, A., and Enge, P., "Validation of the WAAS MOPS Integrity Equation," *Proceedings of the ION Annual Meeting 1999*, Institute of Navigation, Cambridge, MA, 1999, pp. 217–227.

[15] Ibrahim, H. E., and El-Rabbany, A., "Stochastic Modeling of Residual Tropospheric Delay," *ION NTM 2007 on Disc* [CD-ROM], Institute of Navigation, San Diego, CA, 22–24 Jan. 2007.

[16] RTCA Special Committee 159, "Minimum Operational Performance Standards for Global Positioning System/Wide Area Augmentation System Airborne Equipment," Rept. DO-229C, Washington, D.C., 2001.

[17] Bar-Shalom, Y., Rong Li, X., and Kirubarajan, T., *Estimation with Application to Tracking and Navigation*, Wiley–Interscience, New York, 2001.

[18] Manadhar, D., Honda, K., and Murai, S., "Accuracy Assessment and Improvement for Level Survey Using Real Time Kinematic (RTK) GPS," *Proceedings of IEEE 1999 International Geoscience and Remote Sensing Symposium*, Vol. 2, IEEE, Piscataway, NJ, 1999, pp. 882–884.